CFD Analysis of a solar flat plate collector with different cross sections

(Análisis CFD de un colector de placa plana con distintas secciones transversales)

Anthony Xavier Andrade,[1] *William Quitiaquez Sarzosa,*[2] *Luis Fernando Toapanta*[3]

Abstract

Low and medium solar heating systems used for domestic and industrial applications, such as water and space heating, usually utilize solar flat plate collectors in order to absorb solar thermal energy converting it into heat and then transferring the heat to a fluid (usually water or air) that flows through it. The aim of this study is to evaluate the solar flat plate collector's efficiency and the fluid behavior inside the pipeline with three different cross sections, whose hydraulic diameters are 10, 5.12 and 6.16 mm, by using ANSYS Fluent. The results obtained from the Computational Fluid Dynamics (CFD) tool showed that the collector with the Type I cross section reached temperatures up to 330 K at the pipe outlet obtaining an efficiency of 68 %, higher than those of Types II and III, whose efficiencies were 51 % and 60 %, respectively. Type I cross section also presented the lowest values in both speed and pressure drop, these being 0.266 m/s and 108.3 Pa, respectively.

Keywords

Solar collector, cross section, efficiency, ANSYS Fluent, CFD.

Resumen

Los sistemas de calefacción solar utilizados para propósitos industriales y domésticos como sistemas de calentamiento de agua y sistemas de calefacción, generalmente utilizan colectores solares de placa plana para absorber la energía solar térmica convirtiéndola en calor para luego transferir el calor a un fluido (generalmente agua o aire) que circula a través de él. El presente artículo evalúa la eficiencia del colector solar de placa plana, así como el comportamiento del fluido (agua o aire) dentro de la tubería con tres diferentes secciones transversales, cuyos diámetros hidráulicos son 10, 5.12 y 6.16 mm, utilizando ANSYS Fluent. Los resultados obtenidos con herramienta Computational Fluid Dynamics (CFD) mostraron que el colector con la sección transversal Tipo I alcanzó temperaturas de hasta 330 K en la salida de la tubería, obteniendo una eficiencia del 68 %, superior a la de los Tipos II y III, cuyas eficiencias fueron de 51 % y 60 %, respectivamente. La sección transversal del Tipo I también presentó los valores más bajos, tanto en velocidad como en caída de presión, con valores de 0.266 m/s y 108.3 Pa, respectivamente.

Palabras clave

Colector solar, sección transversal, eficiencia, ANSYS Fluent, CFD.

1. Introduction

Due to the environmental crisis and growing demand for energy, the development and implementation of renewable energy has become a matter of great importance. Solar energy is a promising source of energy due to its free availability and low operating costs, along its being a non-polluting source (Li, Liu, Guo, & Zhou, 2017; Kannan & Vakeesan, 2016). Solar energy can be used in solar water heating systems, pool heaters and other heating systems (Ingle, Pawar, Deshmukh, & Bhosale, 2013). Within solar energy systems, the main component is the solar collector, which is a heat exchanger that absorbs and captures incident solar radiation converting

1   Universidad Politécnica Salesiana, Quito-Ecuador (aandradec1@est.ups.edu.ec), https://orcid.org/0000-0002-3494-1963.
2   Universidad Politécnica Salesiana, Quito-Ecuador (wquitiaquez@ups.edu.ec).
3   Universidad Politécnica Salesiana, Quito-Ecuador (ltoapanta@ups.edu.ec).

it into heat and then transferring the heat to a fluid (usually water or air) that flows through the collector.

Although solar flat plate collectors produce lower temperatures, they have the advantage of being simpler in design and having lower maintenance costs and thus are the most used collectors for solar heating systems in the residential and industrial sectors (Ingle, Pawar, Deshmukh & Bhosale, 2013; Birhanu, Ramayya & Shunki, 2016). A typical flat plate collector consists of an insulated metal box with a glass or plastic cover, and a dark-colored absorber plate (Karanth, Madhwesh, Kumar, & Manjunath, 2015), as shown in Figure 1.

Figure 1. Schematic diagram of a flat plate collector. (Mesa, 2006)
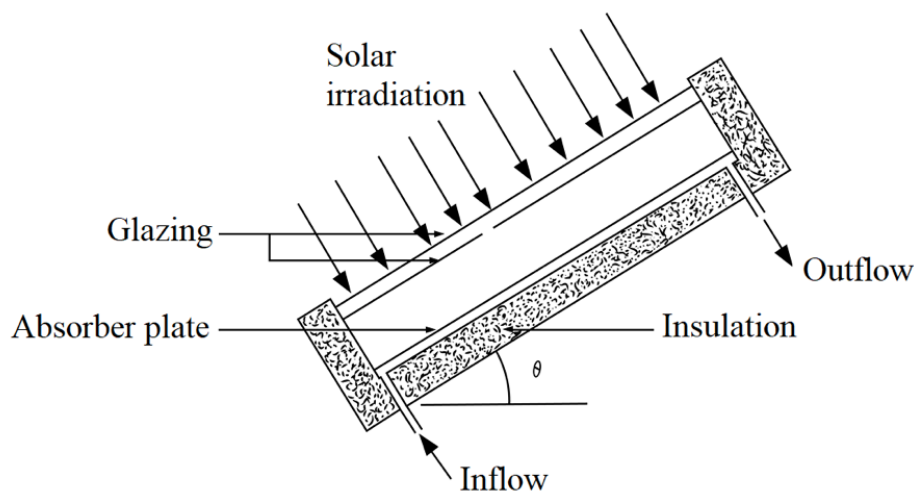
According to Matrawy & Farkas (1997), the configuration of a solar collector is an important factor that determines its thermal performance. A solar collector with a serpentine tube works better than a conventional collector with parallel tubes due to the earlier appearance of turbulent flow that improves the application of heat transfer and increases its maximum efficiency from 62 % to 65 %. Myrna & Beckman (1998) concluded that the internal heat transfer coefficient, which increased approximately 3 % when a serpentine flat plate collector was used, was the main reason for the performance difference between a conventional flat plate collector and a serpentine flat pate collector. Eisenmann, Wiese, Vajen & Ackermann (2000) conducted experiments on two serpentine flat plate collectors, which had the same shape and geometry. In the first collector, the serpentine tube was welded directly to the absorber plate; whilst in the second collector, the serpentine tube and the plate were joined without thermal fusion. Both collectors were placed under the sun in identical weather conditions and their performances were compared. The efficiency of the first collector increased from 2 % to 2.5 %.

Investigations by Prakash, Vishnuprasad & Ramana (2013) and Madhukeshwara & Prakash (2012) showed that the use of special surface coatings improves the optical properties of the collector, the operating temperatures and the performance of the system. Sopian, Syahri, Abdullah, Othman & Yatim (2004) experimentally studied the performance of a new design of solar water heater, where the collector and storage tank were integrated into the same unit. The temperatures registered in the storage tank oscillated between 60 and 63 °C with a radiation of 700 W/m2 and the efficiency of the system was 45 % with an ambient temperature of 31 °C.

Prasad, Byregowda & Gangavati (2010) conducted an experimental study on a water heater with a flat plate collector and a solar tracking mechanism increasing the system's thermal efficiency by 21 %, approximately. Meanwhile, Basavanna & Shashishekar (2013) analyzed a flat plate solar collector with triangular pipes obtaining an increase in the water outflow temperature up to 330 K. Shelke & Patil (2015) analyzed the effect of variations in tube shapes for flat plate solar water heater. They compared the outlet temperature between an elliptical tube and a circular tube, concluding that elliptical tube gives the maximum outlet temperature of water for the same heat flux and inlet temperature. The outlet temperature difference between circular and elliptical tube was 4.17 °C.

Selmi Al-Khawaja & Marafia (2008) simulated and analyzed a flat plate solar collector using a Computational Fluid Dynamics (CFD) software. An experimental model was built and experimental tests were performed to validate the CFD model, obtaining good results. The simulated temperature curve has the same behavior as that experimental one and they are similar. A numerical and experimental investigation of the flow and temperature distribution in a solar collector was performed by Ranjitha, Somashekar, & Jamuna (2013), they investigated the influence of the tube shape and the absorber plate effect on flow and thermal distribution with CFD simulations. The comparison between CFD simulations and the experimental measurements showed only 5 % deviation.

Muhammed & Benny (2015) analyzed the performance of a flat plate solar collector using ANSYS Fluent. They investigated the effect of certain important parameters such as mass flow, material of the absorber plate and variations in the shape of the collector tubes by comparing the inflow and outflow temperature of the fluid. Meanwhile, also using ANSYS Fluent, Mukesh (2016) compared the CFD solutions of different used forms of absorber plates in flat plate collectors. The plate with the best results was selected to be manufactured. They concluded that CFD analysis is an effective tool for researchers to simulate several models in different operating conditions, without manufacturing them comparing their results, saving time and money.

Vasudeva, Manjunath & Yagnesh (2011) analyzed the performance of a flat plate solar collector by using the Discrete Transfer Radiation Model (DTRM). They observed that the heat transfer to the fluid due to solar radiation increased when mass flow rate increased, while the temperature of the absorber plate decreased. Additionally, Marroquin, Olivares, Jiménez, Zamora & Encinas (2013) performed the CFD simulation of two collectors with different cross sections, with a rectangular and a circular cross section. Both showed a temperature increase up to 62.5 °C. The authors also determined the Reynolds number for each collector; collector A presented a variation of 25 < Re < 115, whilst collector B showed a variation of 200 < Re < 225, concluding that collector B was the most efficient since it presented a more uniform flow.

There are not a lot of investigations about cross sections of the solar collector, through which the fluid flows, the selected sections were chosen according to a thermal analysis. CFD model proposed in the present investigation was validated with the simulation performed by Gunjo, Mahanta & Robi (2017) in their research entitled "CFD and experimental investigation of flat solar water heating system under steady state condition". Figure 2 shows the used process to carry out the presented investigation.

The aim of this study is to investigate the effect of operating parameters on the performance of a solar flat plate collector with different cross sections component of a direct expansion solar assisted heat pump (DX-SAHP). A mathematical description of the system governing equations is presented, and the effect of different cross sections was analyzed.

Figure 2. Flow chart of the CFD simulation
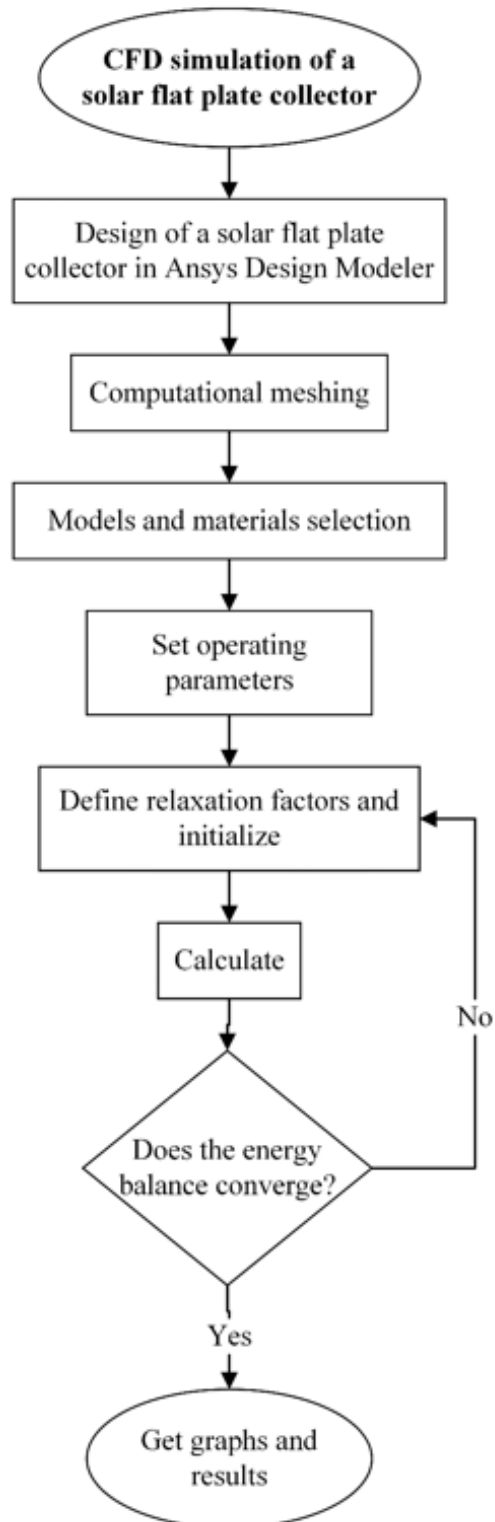
2. Numerical modelling

This study analyzed three geometries for the cross section of a pipe of a conventional flat plate collector, as shown in Figure 3. The behavior of the fluid and performance of the solar collector are studied using the three configurations.

Figure 3. Types of cross sections

| $D_h = 10mm$ | $D_h = 5.12mm$ | $D_h = 6.16mm$ |
| Type I | Type II | Type III |
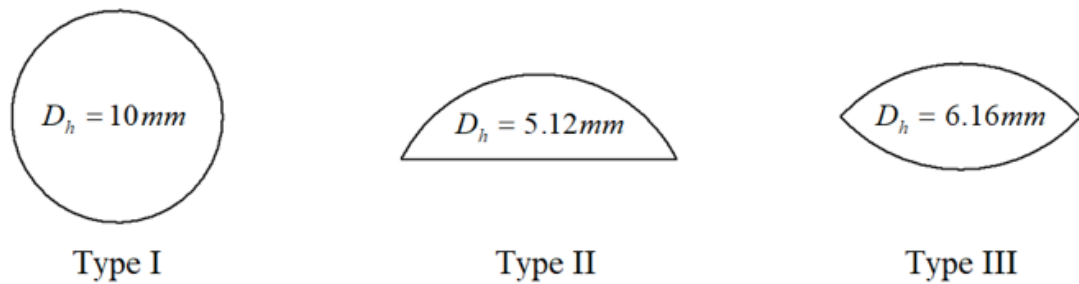
2.1. Governing equations

For the CFD analysis, ANSYS Fluent 16 was used to determine the water outflow temperature, as well as the heat distribution in the plate by solving the equations of continuity, momentum and energy (ANSYS Fluent Theory Guide 12.0, 2009; ANSYS Fluent User Guide, 2012):

- Continuity equation

$$\frac{\partial \rho}{\partial t} + \nabla \cdot (\rho \vec{v}) = S_m$$

(1)

The source Sm is the added mass to the continuous phase from the second dispersed phase.

- Moment equation

$$\frac{\partial}{\partial t}(\rho \vec{v}) + \nabla \cdot (\rho \vec{v} \vec{v}) = -\nabla_p + \nabla \cdot (\bar{\bar{\tau}}) + \rho \vec{g} + \vec{F}$$

(2)

Where $\bar{\bar{\tau}}$ is the stress tensor:

$$\bar{\bar{\tau}} = \mu \left[\left(\nabla \vec{v} + \nabla \vec{v}^T \right) - \frac{2}{3} \nabla \cdot \vec{v} I \right]$$

(3)

- Energy equation

$$\frac{\partial}{\partial t}(\rho E) + \nabla \cdot (\vec{v}(\rho E + p)) = \nabla \cdot \left(k_{\mathit{eff}} \nabla T - \sum_j h_j \vec{J}_j + \left(\overline{\overline{\tau}}_{\mathit{eff}} \cdot \vec{v} \right) \right) + S_h$$

(4)

In Equation 4,

$$E = h - \frac{p}{\rho} + \frac{v^2}{2}$$

(5)

2.2. Computational domain

The length, width and thickness measurements of the collector are 1.6, 0.1 and 0.001 m, respectively, whilst the dimensions of the pipe cross section vary according to the type of the used section. Table 1 shows the main characteristics of the collector used in this investigation.

Table 1. Collector specifications

Description	Specification
Length of absorber plate	1.6 m
Width of absorbent plate	0.1 m
Thermal conductivity of absorber plate	387.6 W/m-K
Density of plate material	8954 kg/m^3
Plate thickness	0.001 m
Pipeline thickness	0.001 m

Domain discretization was done considering a structured grid consisting of hexahedral elements of 0.8 mm for the fluid part and 1 mm for the solid part. The number of registered elements in the mesh for the computational domain consisting of water, water pipe and absorber plate are 523200 for Case I, 425780 for Case II and 515088 for Case III. Figure 4 shows the used 3D meshes for the different sections, as well as their skewness and their element quality.

Figure 4. Computational meshing
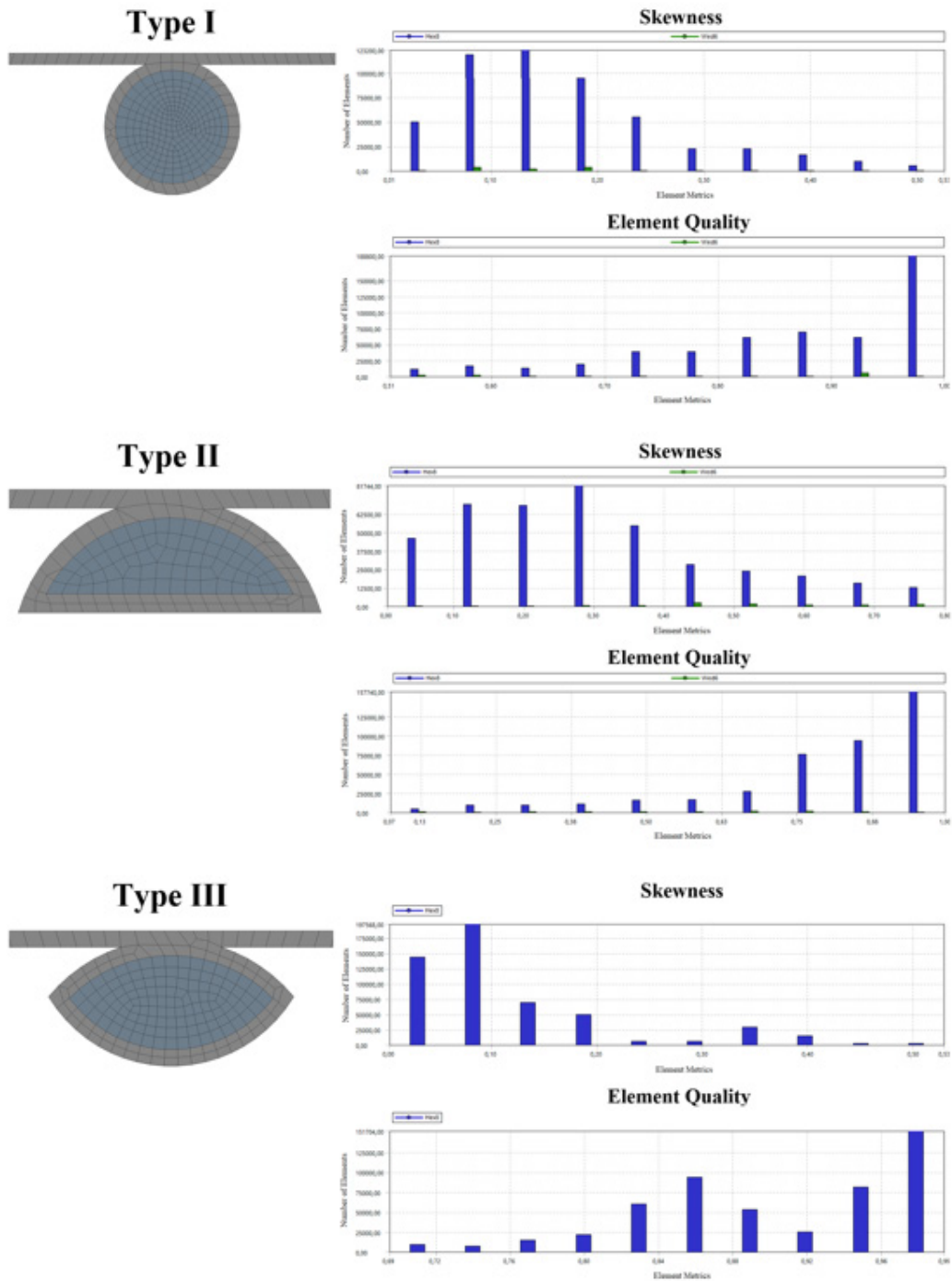
2.3. Simulation conditions

The analysis was carried out based on the following assumptions:

- The physical and thermal properties of the absorber plate, pipe and water are independent of the temperature.
- Water is a continuous and incompressible.
- The flow is stable and has characteristics of laminar flow.
- The heat loss from the bottom of the plate and the tube is by convection, which depends upon wind speed

A constant heat flux (solar radiation) is applied to the upper part of the plate, whilst the lower part is established as a convective surface where the convective heat transfer coefficient is obtained by (Gunjo et al., 2017):

$$h_{conv} = 2.8 + 3\,v_w \qquad (6)$$

Where:

h_{conv} Convective heat transfer coefficient, W/m²-K

v_w Wind speed, m/s

The efficiency of the solar collector is determined by:

$$\eta = \frac{\dot{m}\,c_p\,(T_o - T_i)}{I\,A_c} \qquad (7)$$

Where:

$\dot{m}$ Mass flow of fluid, kg/s

c_p Specific heat of the fluid, J/kg-K

T_i Fluid inflow temperature, K

T_o Fluid outflow temperature, K

I Solar radiation, W/m²

A_c Effective area of the collector, m²

The parameters of solar radiation, ambient temperature, water inflow temperature and mass flow used in the computational model are shown in Table 2.

Table 2. Operating parameters

Parameter	Value
Solar radiation	1200 W/m²
Mass flow	0.0125 kg/s
Room temperature	310 K
Water inflow temperature	305 K
Wind speed	2 m/s

3. Results and discussion

Figures 5, 6 and 7 show the temperature variation in (i) the upper part of the plate, (ii) the pipe outflow, and (iii) along the water pipe divided in sections, obtained from the CFD simulation.

Figure 5. Temperature variation in the upper part of the plate
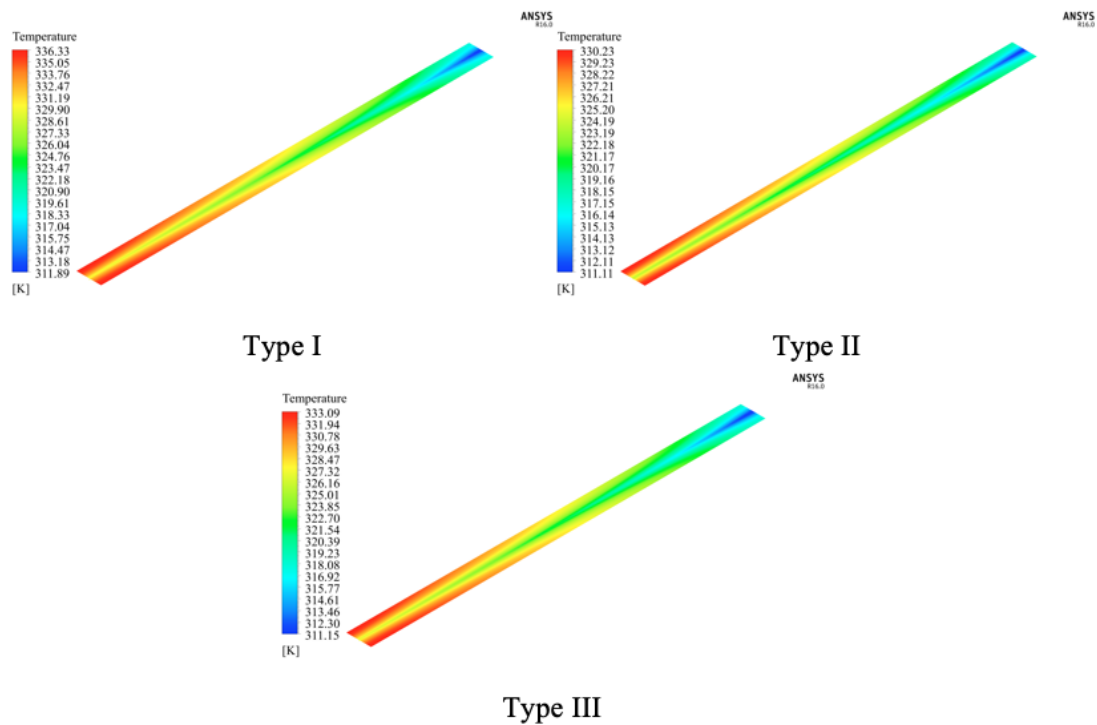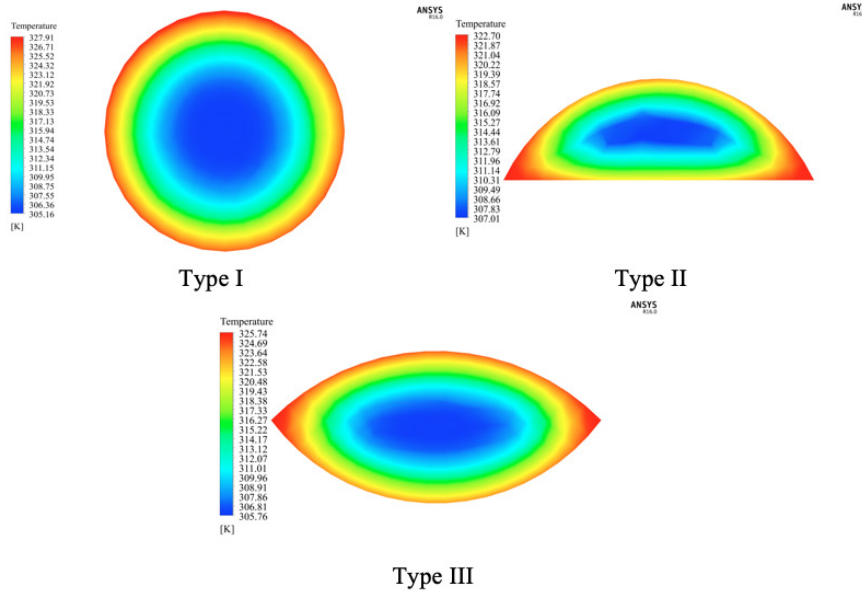

Type I

Type II

Type III

Figure 5 shows the temperature variation in the upper part of the absorber plate for each of the different cross sections. The absorber plate with Type I cross section obtained a variation of 25 K, whilst the plates with Type II and Type III cross sections showed a variation of 19 and 22 K, respectively. This is because the fluid that flows through the pipe absorbs some of the heat from the absorber plate, which causes these temperature differentials.

Figure 6. Temperature variation of the water at the pipe outflow

Type I

Type II

Type III

Temperature distribution at the pipe outflow for the different sections is presented in Figure 6. The solar collector with the Type II cross section had the most uniform temperature distribution as it obtained a variation of only 15 K, followed by the Type III and Type I cross section, with a variation of 20 and of 22 K, respectively.

Figure 7. Temperature variation of the water along the pipe
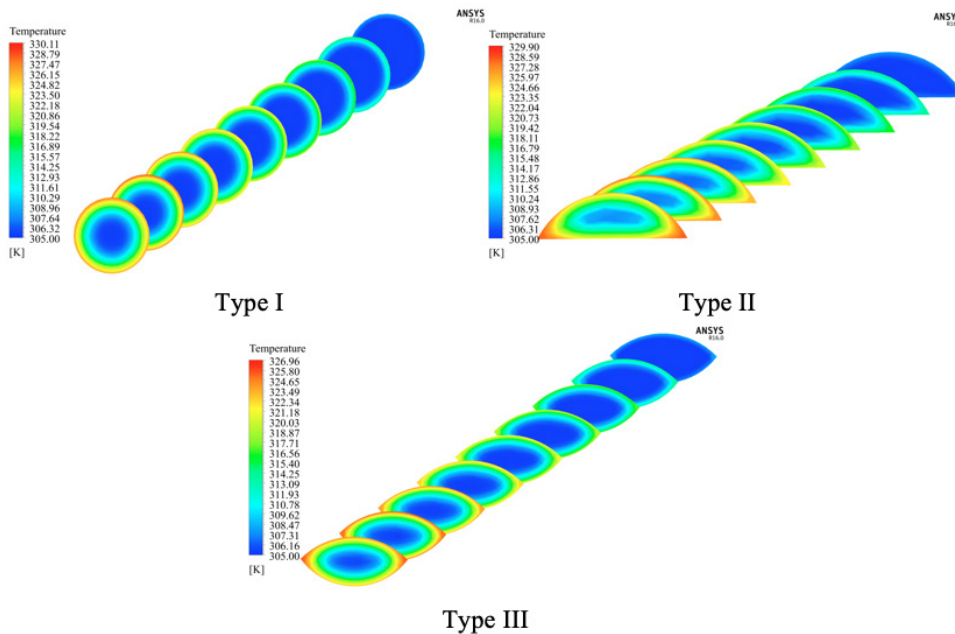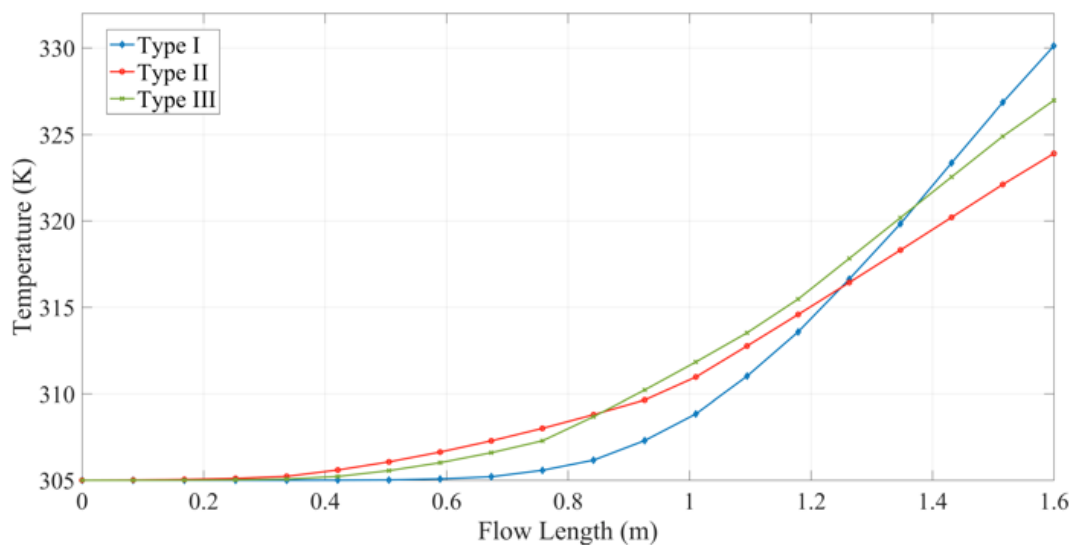

Type I

Type II

Type III

Figure 7 shows the temperature variation of the water along nine different sections of the pipe. The working fluid increases its temperature as it circulates through the pipe. In these three cases, the external part of each geometry presents the higher temperature due to this part is in direct contact with the inner part of the pipe, which permits to absorb greater amount of heat. The fluid into the Type I cross section got the highest temperatures among all of the three sections, reaching values up to 330 K at the pipe outflow.

Figure 8. Variation in fluid temperature

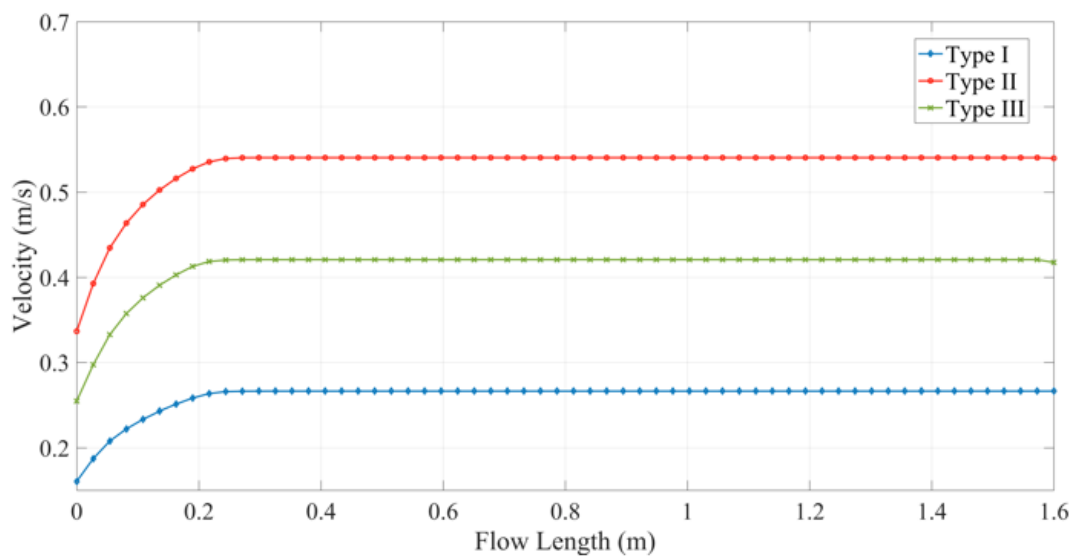**Figure 9.** Fluid pressure drop
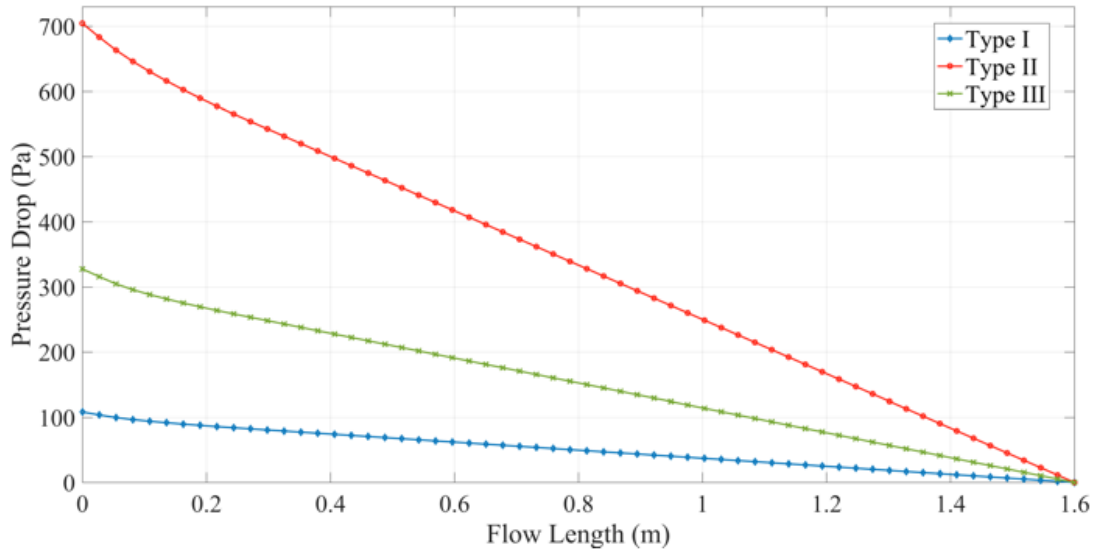
Figure 10. Variation of fluid speed

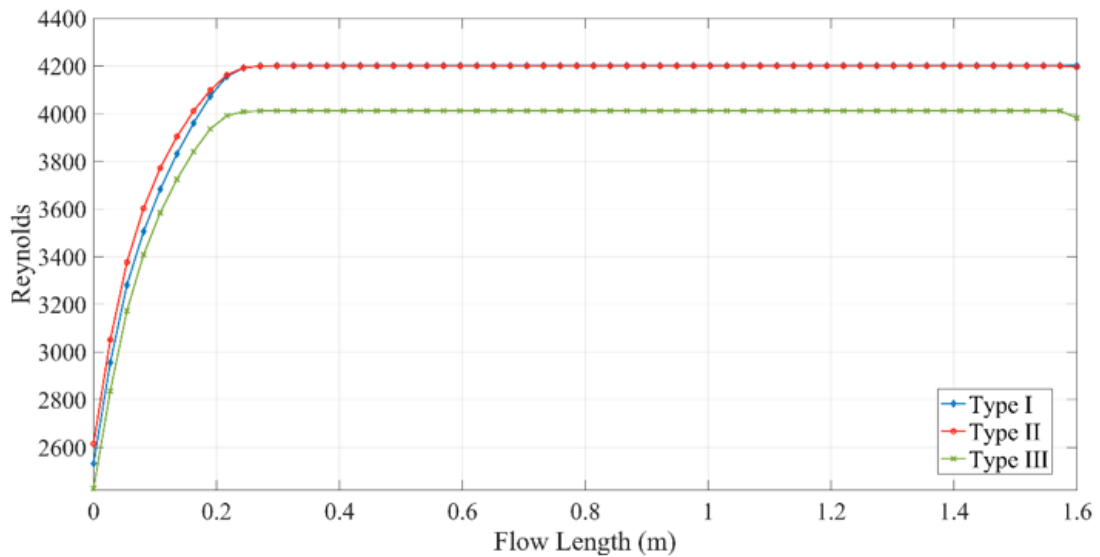Figure 11. Variation of Reynolds number

Figure 8 shows the temperature variation of water along the pipe. The collector with a Type I cross section had the best performance due to it presented the lowest speeds, as shown in Figure 10, which decreased the pressure drop (Figure 9) and improved the heat transfer from the environment to the fluid. Meanwhile, the collectors with Type II and Type III cross sections obtained maximum temperatures of 323.9 and 326.96 K, respectively. The variation of fluid speed also affects the Reynolds number (Figure 11). Type I and Type II present similar Reynolds

number despite of their difference between their velocities and hydraulic diameters, obtaining a value of 4200, while Type III presents a Reynolds number of 4011.

4. Conclusions

The CFD results of the solar flat plate collector with different cross sections, simulated under the same operation conditions and in a steady state showed that the collector with the Type I cross section had the best performance, where the fluid reached temperatures up to 330 K at the pipe outflow and obtaining an efficiency of 68 %, higher than Type II and Type III, which presented efficiencies of 51 and 60 %, respectively. In addition, this cross section presented the lowest values in both speed and pressure differential, 0.266 m/s and 108.3 Pa respectively. However, the collector with the Type II cross section was the one that presented a more uniform temperature distribution at the pipe outflow, obtaining a variation of only 15 K, followed by the Type III and the Type I with a variation of 20 and 22 K, respectively.

References

ANSYS Fluent Theory Guide 12.0. (2009, Abril).

ANSYS Fluent User Guide. (2012, Noviembre).

Basavanna, S., & Shashishekar, K. (2013). CFD Analysis of triangular absorber tube of a solar flat plate collector. *International Journal of Mechanical Engineering and Robotics Research, 2* (1): 19-24.

Birhanu, G., Ramayya, A. & Shunki, G. (2016). Computational Fluid Dynamic Simulation and Experimental Testing of a Serpentine Flat Plate Solar Water Heater. *International Journal of Scientific & Engineering Research, 7* (10): 320-333.

Eisenmann, W., Wiese, F., Vajen, K. & Ackermann, H. (2000). Experimental investigations of serpentine-flow flat-plate collectors. *Philipps-Universität Marburg, D-35032 Marburg, Germany.*

Gunjo, D. G., Mahanta, P. & Robi, P. S. (2017). CFD and experimental investigation of flat plate solar water heating system under steady state condition. *Renewable Energy,* 106: 24-36.

Ingle, P., Pawar, A., Deshmukh, B. & Bhosale, K. (2013). CFD Analysis of Solar Flat Plate Collector. *International Journal of Emerging Technology and Advanced Engineering, 3* (4): 337-342.

Kannan, N., & Vakeesan, D. (2016). Solar energy for future world: -A review. *Renewable and Sustainable Energy Reviews,* 62: 1092-1106.

Karanth, K., Madhwesh, N., Kumar, S. & Manjunath, M. (2015). Numerical and experimental study of a solar water heater for enhancement in thermal performance. *International Journal of Research in Engineering and Technology, 4* (3): 548-553.

Li, Q., Liu, Y., Guo, S. & Zhou, H. (2017). Solar energy storage in the rechargeable batteries. *Nano Today,* 16: 46-60.

Madhukeshwara, N. & Prakash, E. (2012). An investigation on the performance characteristics of solar flat plate collector with different selective surface coatings. *International Journal of Energy & Environment,* 3: 99-108.

Marroquín-De Jesús, Á., Olivares-Ramírez, J. M., Jiménez-Sandoval, O., Zamora-Antuñano, M. A. & Encinas-Oropesa, A. (2013). Analysis of Flow and Heat Transfer in a Flat Solar Collector with Rectangular and Cylindrical Geometry Using CFD. *Ingeniería Investigación y Tecnología, 14* (4): 553-561.

Matrawy, K. K. & Farkas, I. (1997). Comparison study for three types of solar collector for water heating. *Energy Conversion and Management,* 38: 861–869.

Mesa, F. (2006). *Colector solar de placa plana.* Bogotá: Energía Solar.

Muhammed Yarshi, K. A. & Benny, P. (2015). Analysis of Heat Transfer Performance of Flat Plate Solar Collector using CFD. *International Journal of Science, Engineering and Technology Research, 4* (10): 3576-3580.

Mukesh Manilal, K. (2016). Design, CFD Analysis and Fabrication of Solar Flat Plate Collector. *International Research Journal of Engineering and Technology*, 3 (1): 1000-1004.

Myrna, D. K. S., & Beckman, W. (1998). Analysis of serpentine collectors in low flow systems. *Solar Energy Laboratory University of Wisconsin-Madison 1500 Engineering Drive Madison, WI 53706*.

Prakash, B., Vishnuprasad, B. & Ramana, V. (2013). Performance study on effect of nano coatings on liquid flat plate collector: An experimental approach. *International Journal of Mechanical Engineering and Robotics Research, 2* (4): 379-384.

Prasad, P., Byregowda, H. & Gangavati, P. (2010). Experiment Analysis of Flat Plate Collector and Comparison of Performance with Tracking Collector. *European Journal of Scientific Research, 40* (1): 144-155.

Ranjitha, P., Somashekar, V. & Jamuna, A. (2013). Analysis of Solar Flat Plate Collector for Circular Pipe Configuration by using CFD. *International Journal of Engineering Research & Technology (IJERT), 2*(12), 3356-3362.

Selmi, M., Al-Khawaja, M. & Marafia, A. (2008). Validation of CFD simulation for flat plate solar energy collector. *Renewable Energy, 33* (3): 383-387.

Shelke, V., & Patil, C. (2015). Analyze the Effect of Variations in Shape of Tubes for Flat Plate Solar Water Heater. *International Journal of Scientific Engineering and Research (IJSER), 3* (4): 118-124.

Sopian, K., Syahri, M., Abdullah, S., Othman, M. & Yatim, B. (2004). Performance of a non-metallic unglazed solar water heater with integrated storage system. *Renewable Energy, 29* (9): 1421-1430.

Vasudeva Karanth, K., Manjunath, M. & Yagnesh Sharma, N. (2011). Numerical Simulation of a Solar Flat Plate Collector using Discrete Transfer Radiation Model (DTRM) – A CFD Approach. *Proceedings of the World Congress on Engineering, 3*.